Modified Fresnel computer-generated hologram directly recorded by multiple-viewpoint projections

Natan T. Shaked* and Joseph Rosen

Department of Electrical and Computer Engineering, Ben-Gurion University of the Negev, P.O. Box 653, Beer-Sheva 84105, Israel

*Corresponding author: natis@ee.bgu.ac.il

Received 15 October 2007; accepted 30 November 2007;
posted 11 December 2007 (Doc. ID 88603); published 8 February 2008

An efficient method for obtaining modified Fresnel holograms of real existing three-dimensional (3-D) scenes illuminated by incoherent white light is presented. To calculate the hologram, the method uses multiple-viewpoint projections of the 3-D scene. However, contrary to other similar methods, this one is able to calculate the Fresnel hologram of the 3-D scene directly rather than calculating a Fourier hologram first. This significantly decreases the amount of calculations needed to obtain the hologram and also reduces the reconstruction errors. The proposed method is first mathematically introduced and then demonstrated by both simulations and experiments. © 2008 Optical Society of America

OCIS codes: 090.0090, 090.1760, 100.6890, 110.6880.

1. Introduction

Multiple-viewpoint projection (MVP) holograms were first proposed by Li *et al.* [1] and further developed by Abookasis and Rosen [2] and Sando *et al.* [3]. The principle behind these methods is the acquisition of multiple projections of a three-dimensional (3-D) scene from various viewpoints. These projections are processed in the computer to yield a hologram of the scene which is, unlike the composite hologram [4], equivalent to an optical hologram of the same scene recorded from a single point of view. Using these methods, it is possible to obtain holograms with a simple digital camera, operating under conditions of incoherent white light illumination and without most of the disadvantages characterizing conventional holography, i.e., the need for a powerful, highly coherent light source, typically a laser, and extreme stability of the optical system. MVP holograms can be reconstructed optically by illuminating the hologram with a coherent plane wave, or alternatively, by using a digital reconstruction technique. Several kinds of MVP hologram appear in the literature, such as image holograms [5], Fourier holograms [1,2,5], Fresnel–Fourier holograms [5], and Fresnel holograms [3,5].

One disadvantage of MVP holograms is the complication of acquiring the large number of viewpoint projections of the 3-D scene needed to generate a high-resolution hologram. Another difficulty is the numerical complexity and the inaccuracy of the digital process carried out on the acquired projections.

We have recently proposed two different methods to make the projection acquisition more efficient. In the first method, we use a microlens array for acquiring the entire viewpoint projections of the 3-D scene in a single camera shot [6]. In the second method, we acquire only a small number of extreme projections and predict the middle projections in the computer by use of the view synthesis algorithm [7]. Sando *et al.* [8] proposed another method for decreasing the number of projections by scanning the scene along various transverse curvatures.

In the present study, we tackle the second problem mentioned above, namely, the numerical complexity and inaccuracy of the digital process performed on the acquired projections. We present a new and direct method to synthesize a modified Fresnel hologram using the MVPs. In [3] and [5], the generation of the MVP Fresnel hologram was performed indirectly, by a convolution between the digital reconstructed images of an MVP Fourier hologram and the quadratic phase functions. This process is approximated, inaccurate, and requires redundant calculations that can be avoided by using the new direct method proposed herein.

0003-6935/08/1900D21-7$15.00/0

Avoiding redundant calculations reduces digital errors during the various transformations. Moreover, the proposed direct Fresnel holography method does not use approximations, such as the small angle assumption used for the Fourier and other types of hologram. Therefore, the direct Fresnel holograms are not limited to small angles and hence their reconstructions are more accurate than in the other holograms. Avoiding redundant calculations becomes extremely critical when Fresnel holograms with a large number of pixels have to be calculated. In addition, as stated in our previous papers, the prospective goal of these white light holography methods is the design of a portable digital holographic camera. For such a camera (especially for a video camera generating holograms in real time), it is important to use as few digital calculations as possible.

The method proposed in this paper is first mathematically introduced in Section 2, and its equivalence to an optical recording process is discussed in Section 3. Simulation and experimental results are described in Sections 4 and 5, respectively.

2. Description of the Method

Figure 1 illustrates the optical system used for acquiring multiple projections of the 3-D scene. Each time the digital camera moves to a different location and acquires a single projection of the 3-D scene. Note that other acquisition methods, such as spatial multiplexing of cameras or using a microlens array to capture the entire projection of the 3-D scene in a single camera shot [6], are also possible.

Assuming that $2K + 1$ projections of the 3-D scene are acquired along the horizontal axis only, we number the projections by m, so that the middle projection is denoted by $m = 0$, the right projection by $m = K$, and the left projection by $m = -K$. Let $P_m(x_p, y_p)$ be the mth projection, where x_p and y_p are the axes on the projection plane. According to the proposed method, the mth projection $P_m(x_p, y_p)$ is multiplied by a 1-D quadratic phase function and the result is summed to the (m, n)th pixel in the final matrix as follows:

$$H(m,\ n) = \int\int P_m(x_p,\ y_p) E_n(x_p,\ y_p) dx_p dy_p, \quad (1)$$

where $E_n(x_p, y_p)$ represents the 1-D quadratic phase function defined as

$$E_n(x_p,\ y_p) = \exp(-j2\pi b x_p^2)\delta(y_p - n\Delta p), \quad (2)$$

where b is an adjustable parameter, δ is the Dirac delta function, and Δp is the pixel size of the digital camera.

The process described by Eqs. (1) and (2) is repeated for all the projections, so that each projection contributes a different column to the final matrix $H(m, n)$. As shown in Section 3, in the end of the process, the obtained 2-D complex matrix $H(m, n)$ represents the 1-D modified Fresnel hologram of the observed scene.

3. Equivalence to an Optical Fresnel Hologram

In this section we show that the 2-D complex function, obtained from the multiple projections according to Eqs. (1) and (2) indeed represents the 1-D modified Fresnel hologram of the observed 3-D scene. In fact, the obtained computer-generated hologram is almost equivalent to an optical 1-D Fresnel hologram recorded from a single point of view, and not just any point of view, but from the central point of view.

Let us define the relation between an arbitrary point on the 3-D object and its projected point on the mth projection plane $P_m(x_p, y_p)$. Figure 2 illustrates a top view of the optical system shown in Fig. 1. By using simple geometric relationships for the quantities illustrated in Fig. 2, the coordinates of the projection plane are

$$x_p = \frac{f(x_s - m\alpha)}{z_s}, \qquad y_p = \frac{f y_s}{z_s}, \quad (3)$$

where x_s, y_s and z_s are the axes of the 3-D scene, f is the focal length of the imaging lens, and α is the camera (and the imaging lens) movement between two adjacent projections. Let us look at a single source point (SSP), with an infinitesimal size of $(\Delta x_s, \Delta y_s, \Delta z_s)$, located on the 3-D scene at coordinates (x_s, y_s, z_s) and having a value of $h(x_s, y_s, z_s)$. Using Eq. (1), the complex amplitude distribution obtained on the hologram plane by this source point is

$$\begin{aligned} H_{\mathrm{SSP}}(m,\ n;\ x_s,\ y_s,\ z_s) &= \int\int [h(x_s,\ y_s,\ z_s)\Delta x_s \Delta y_s \Delta z_s \\ &\quad \times \delta(x_p' - x_p,\ y_p' - y_p)] \\ &\quad \times E_n(x_p',\ y_p') dx_p' dy_p' \\ &= h(x_s,\ y_s,\ z_s) E_n(x_p,\ y_p) \\ &\quad \times \Delta x_s \Delta y_s \Delta z_s. \end{aligned} \quad (4)$$

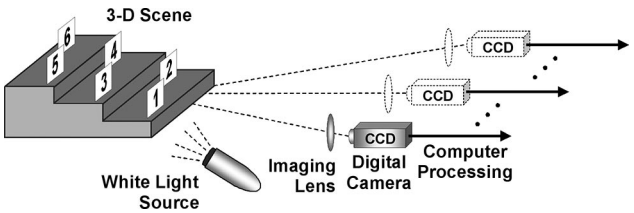

Fig. 1. Optical system for capturing multiple-viewpoint projections of the 3-D scene. The camera and its imaging lens move together into a different capturing viewpoint for each projection.

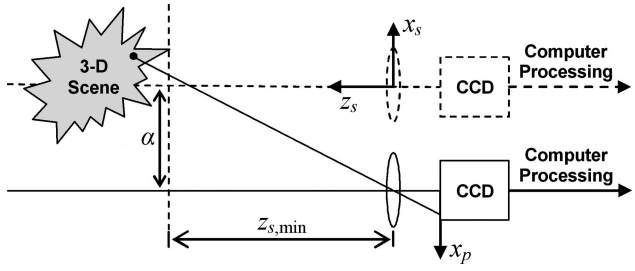

Fig. 2. Top view of the optical system shown in Fig. 1.

By substituting Eqs. (2) and (3) into Eq. (4), the complex amplitude distribution becomes

$$H_{\mathrm{SSP}}(m,\ n;\ x_s,\ y_s,\ z_s) = h(x_s,\ y_s,\ z_s) \times \exp\left[-j2\pi bf^2\ \frac{(x_s - m\alpha)^2}{z_s^2}\right] \times \delta\left(\frac{fy_s}{z_s} - n\Delta p\right)\Delta x_s \Delta y_s \Delta z_s. \quad (5)$$

The overall complex amplitude distribution of the hologram resulting from all the 3-D scene points is a volume integral over all the coinciding SSP holograms as follows:

$$\begin{aligned} H(m,\ n) &= \int\int\int H_{SSP}(m,\ n;\ x_s,\ y_s,\ z_s)dx_s dy_s dz_s \\ &= \int\int\int h(x_s,\ y_s,\ z_s)\exp\left[-j2\pi bf^2\ \frac{(x_s - m\alpha)^2}{z_s^2}\right] \\ &\quad \times \delta\left(\frac{fy_s}{z_s} - n\Delta p\right)dx_s dy_s dz_s. \end{aligned} \quad (6)$$

Defining an axial coordinate transformation $z_s' = z_s^2$ (so $dz_s = dz_s'/(2\sqrt{z_s'})$), the hologram complex amplitude distribution is

$$H(m,\ n) = \int\int\int \frac{1}{2\sqrt{z_s'}}\ h(x_s,\ y_s,\ z_s') \times \exp\left[-j2\pi bf^2\ \frac{(x_s - m\alpha)^2}{z_s'}\right] \times \delta\left(\frac{fy_s}{\sqrt{z_s'}} - n\Delta p\right)dx_s dy_s dz_s'. \quad (7)$$

Equation (7) has the similar functional behavior of the complex amplitude distribution of a 1-D digital Fresnel hologram of the 3-D scene [5,9]. However, note that, in spite of this similarity, there are still several differences between a conventional Fresnel hologram and the proposed hologram. These differences are described next.

To get the reconstructed plane $s(m, n; z_r)$, located at an axial distance z_r from the hologram, $H(m, n)$ is digitally convolved with a 1-D quadratic phase function as follows:

$$s(m,\ n;\ z_r) = \left|H(m,\ n) * \exp\left(\frac{j2\pi}{\gamma z_r}\ m^2\right)\right|, \quad (8)$$

where $*$ denotes a 1-D convolution and γ is a constant. From Eqs. (6) and (8), one can see that the axial positions of the objects reconstructed from the hologram are proportional to the square of the coinciding axial positions of the original objects.

To obtain the transverse magnifications M_x and M_y of the proposed hologram, we first rewrite Eq. (6) as follows:

$$H(m,\ n) = \int\int\int h(x_s,\ y_s,\ z_s) \times \exp\left[-j2\pi b\left(\frac{M\alpha}{\Delta p}\right)^2\left(\frac{\Delta p x_s}{\alpha} - m\Delta p\right)^2\right] \times \delta(My_s - n\Delta p)dx_s dy_s dz_s, \quad (9)$$

where $M = f/z_s$ is the magnification of the imaging lens. Equation (9) shows that the hologram is actually a sampling pattern of the scene by two different horizontal and vertical sampling functions, each of which creates a different transverse magnification. Whereas the vertical delta function magnifies the object's vertical size by M, the horizontal quadratic phase function magnifies the object's horizontal size by the constant $\Delta p/\alpha$. To understand the peculiar horizontal magnification, we recall that the distance between two successive samples on the camera plane is $M\alpha$. Hence, the maximum size of the hologram on the horizontal axis is $2KM\alpha$, so the relative horizontal portion of the imaged object from the whole hologram horizontal size is $\bar{x}_s M/(2KM\alpha)$, where $(\bar{x}_s, \bar{y}_s, \bar{z}_s)$ is the size of the original object. Therefore, the actual horizontal size of the sampled imaged object is $2K\ \Delta p\ \bar{x}_s M/(2KM\alpha) = \bar{x}_s \Delta p/\alpha$. Under the assumption that the same proportions of the recorded hologram are retained in the reconstruction process, the horizontal size of the sampled imaged object is equal to the horizontal size of the object reconstructed from the hologram. Using this analysis, we conclude that the resulting transverse magnifications M_x and M_y of the proposed hologram are

$$M_x = \frac{\bar{x}_r}{\bar{x}_s} = \Delta p/\alpha, \quad M_y = \bar{y}_r/\bar{y}_s = M = f/z_s, \quad (10)$$

where $(\bar{x}_r, \bar{y}_r, \bar{z}_r)$ is the size of the reconstructed object. From Eqs. (10) one can see that, contrary to a conventional Fresnel hologram and to the vertical magnification M_y, the horizontal magnification M_x is constant and is not dependent on the axial positions of the objects in the 3-D scene. This effect can be eliminated by resampling the reconstructed planes along the horizontal axis by M/M_x, as demonstrated in Sections 4 and 5.

The axial magnification M_z of the proposed hologram is calculated by looking at a hologram of an object with the axial size of $\bar{z}_s$, located from z_s to $z_s + \bar{z}_s$. Reconstructing this hologram by Eq. (8) and dividing the axial size of the reconstructed object $\bar{z}_r$ by the axial size of the original object $\bar{z}_s$ yields the value of the axial magnification. Mathematically, the exponent arguments of Eqs. (6) and (8) are equated for two axial points as follows: $1/[\gamma(z_r + \bar{z}_r)] = bf^2\alpha^2/(z_s + \bar{z}_s)^2$ and $1/(\gamma z_r) = bf^2\alpha^2/z_s^2$. Then, combining these two equations yields

$$\bar{z}_r = \frac{1}{\gamma b f^2 \alpha^2}\,\bar{z}_s(\bar{z}_s + 2z_s). \tag{11}$$

Therefore, the resulting axial magnification is

$$M_z = \frac{\bar{z}_r}{\bar{z}_s} = \frac{\bar{z}_s + 2z_s}{\gamma b f^2 \alpha^2}. \tag{12}$$

We conclude that this unique hologram has a nonlinear axial magnification, which can be approximated to a linear axial magnification of $M_z = 2z_s/(\gamma b f^2 \alpha^2)$ for objects of a small axial size. However, even the approximated linear axial magnification behaves differently from the axial magnification of the conventional Fresnel hologram, which is squarely dependent on the transverse magnification of this hologram. Nevertheless, reconstructing the proposed hologram along the transformed axial coordinate $z_r' = z_r^2$ makes the axial magnification of the proposed hologram similar to that of the conventional Fresnel hologram, at least for objects that are not too long ($\bar{z}_s \ll z_s$). Equation (11) is experimentally tested at the end of Section 5.

The adjustable parameter b in Eq. (2) is determined so that the closest point in the 3-D scene will be sampled on the most extreme cycle of the quadratic phase function. Otherwise, the high frequency of the quadratic phase function is not effective in the resulting hologram. The horizontal axis of the hologram extends between $\pm K M_{\max}\alpha = \pm K f \alpha / z_{s,\min}$, where $M_{\max}$ is the maximum value of the magnification and $z_{s,\min}$ is the distance between the imaging lens and the closest point of the 3-D scene. Therefore, under the assumptions that every projection contributes exactly one pixel to the hologram and that the final number of pixels in the hologram is equal to the number of pixels of each of the perspective projections, parameter b should satisfy the following condition:

$$\begin{aligned} b &= [(Kf\alpha/z_{s,\min})^2 - (Kf\alpha/z_{s,\min} - f\alpha/z_{s,\min})^2]^{-1} \\ &\approx z_{s,\min}^2/(2Kf^2\alpha^2). \end{aligned} \tag{13}$$

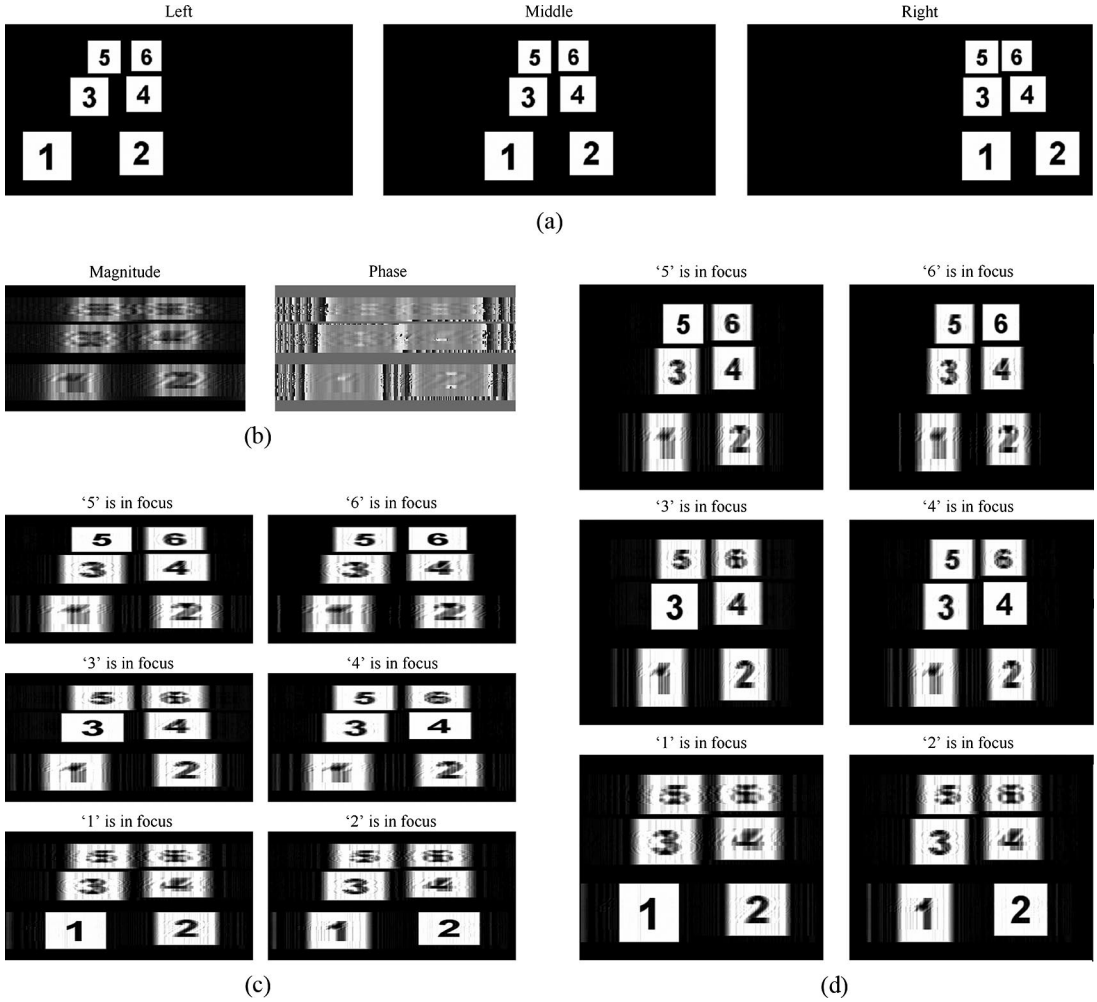

Fig. 3. Simulated results for generating a 1-D modified Fresnel hologram: (a) Several projections taken from the entire digitally obtained projection set, (b) magnitude and phase of the 1-D modified Fresnel hologram, (c) the six best in-focus reconstructed planes along the optical axis, (d) the six best in-focus reconstructed planes along the optical axis after the resampling process of the horizontal axis.

The transverse minimal distance Δx_s that can be resolved by the proposed optical system is determined as the worst (maximum) value between the resolved distance of the imaging system according to the Rayleigh resolution limit, the detector pixel size, and the length of the most extreme cycle of the quadratic phase function given by Eq. (2), where the last two resolution limits are projected onto the object domain. Therefore, the transverse minimal distance that can be resolved by the optical system is

$$\Delta x_s = \max\left\{\frac{1.22\lambda z_s}{D}, \frac{\Delta p}{M}, \frac{f\alpha}{Mz_{s,\min}}\right\}, \tag{14}$$

where λ is the average wavelength used ($\lambda \approx 0.5\ \mu$m) and D is the diameter of the imaging lens. The axial minimal resolved distance Δz_s is determined by projecting Δz_s on the transverse object plane of the most extreme projection in the projection set, which yields

$$\Delta z_s = \Delta x_s z_s/(K\alpha). \tag{15}$$

4. Simulation Results

To test the proposed method, we simulated the generation of a 1-D MVP modified Fresnel hologram. For this purpose, the optical system shown in Fig. 1 was modeled in the computer. The 3-D scene shown in Fig. 1 was composed of six equal-size planes positioned on a dark background. On each plane, a different digit, 1 to 6, was displayed, where the closest plane contained the digit 1 and the farthest plane contained the digit 6. To generate the hologram by simulation, we first digitally synthesized a set of projection planes, each from a different viewpoint of the 3-D scene. Figure 3(a) shows three chosen projections

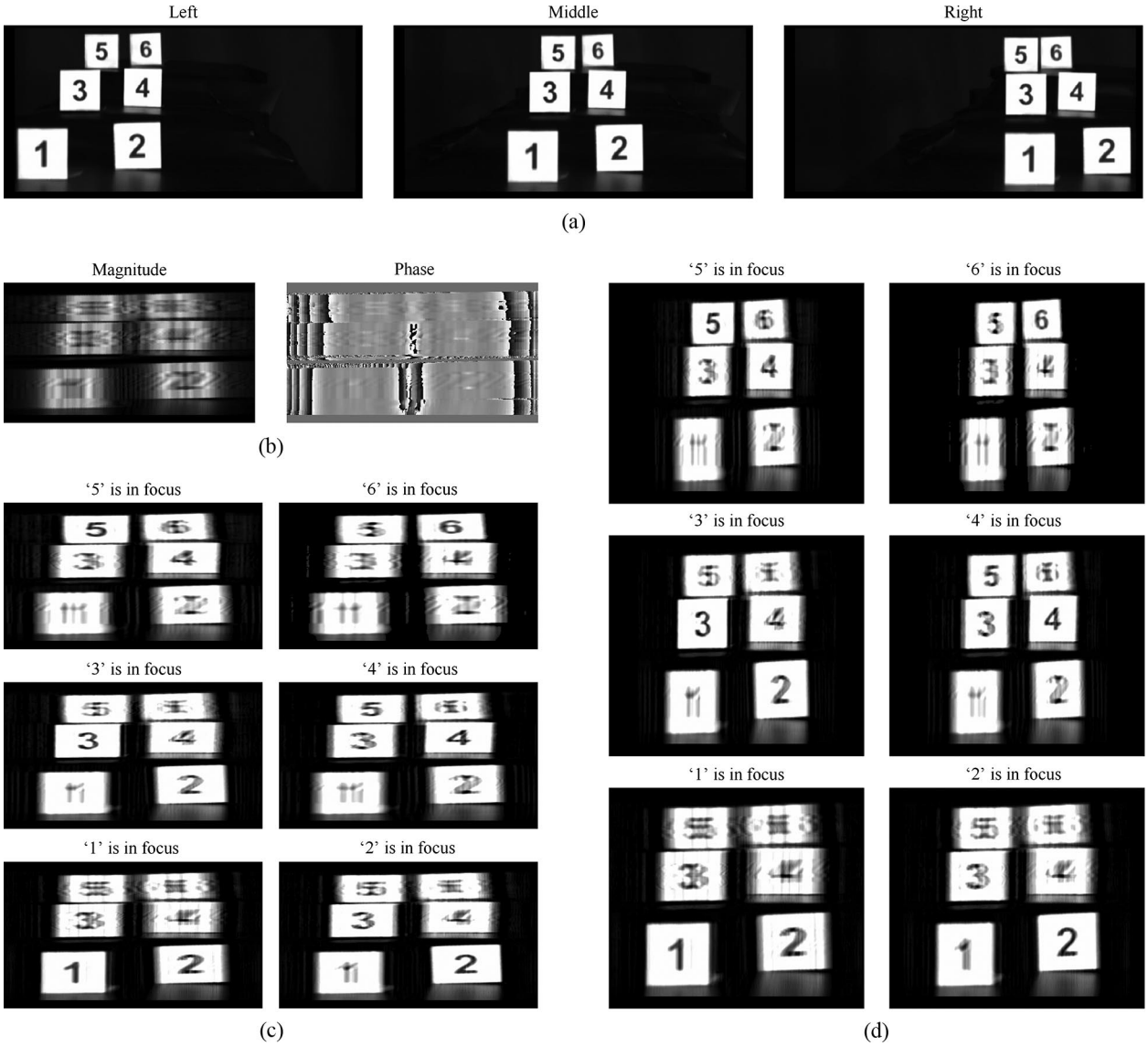

Fig. 4. Experimental results for generating a 1-D modified Fresnel hologram: (a) Several projections taken from the entire experimentally obtained projection set, (b) magnitude and phase of the 1-D modified Fresnel hologram, (c) the six best in-focus reconstructed planes along the optical axis, (d) the six best in-focus reconstructed planes along the optical axis after the resampling process of the horizontal axis.

taken from the entire set of 500 projections generated in the computer. Since these projections were processed into a 1-D Fresnel hologram, the vertical positions of the digits were constant, whereas their horizontal positions were changed according to the parallax effect and the viewpoint.

Each projection was then multiplied, according to Eqs. (1) and (2) by a 1-D quadratic phase function, and the product was summed to a single column in a 2-D complex matrix representing the 1-D modified Fresnel hologram of the 3-D scene. Figure 3(b) shows the magnitude and the phase of the hologram generated from the simulated projections as described above.

To reconstruct the plane $s(m, n; z_r)$ located at a distance z_r from the hologram on the optical axis, the hologram $H(m, n)$ was digitally convolved with a 1-D quadratic phase function according to Eq. (8). Figure 3(c) shows six chosen reconstruction planes along the optical axis obtained by reconstructing the hologram presented in Fig. 3(b). As shown in Fig. 3(c), in each one of the six planes, a different digit is in focus, whereas the other five digits are out of focus. This indicates that volumetric information is indeed encoded into the hologram and therefore the proposed method generates a 1-D Fresnel hologram of the 3-D scene.

According to Eq. (10), the transverse magnification M_x on the horizontal axis is constant. Consequently, all originally equal reconstructed objects (closer and farther) have the same size on the horizontal axis, whereas on the vertical axis the magnification is $M = f/z_s$, so farther objects seem smaller. Therefore, a resampling process by M/M_x on the horizontal axis was applied to the reconstructed planes, so that the original aspect ratios of different objects in the 3-D scene were retained. Figure 3(d) shows each of the six, resampled, best in-focus reconstruction planes in which the aspect ratios of different in-focus reconstructed objects fit the aspect ratios of the coinciding original objects. Note that, since M is inversely proportional to z_s and consequently to $\sqrt{z_r}$, the resampling was different for each and every reconstruction plane.

5. Experimental Results

We now experimentally demonstrate the generation of the proposed hologram by the optical system illustrated in Fig. 1. Six planes, each 2.5 cm × 2.5 cm, containing digits 1–6, were positioned on a dark background and used as the 3-D scene. The distances between the plane containing the digit 1 and the planes containing the digits 2, 3, 4, 5, and 6 were 4, 0, 4, 0, and 4 cm on the horizontal x_s axis; 0, 3.5, 3.5, 6.5, and 6.5 cm on the vertical y_s axis; and 5, 12, 17, 23.5, and 28.5 cm on the optical z_s axis, respectively. The distance between the closest plane containing the digit 1 and the imaging lens was 43 cm. The camera used was a CCD camera (PCO, Scientific 230XS) containing 1280 × 1024 pixels and an 8.6 mm × 6.9 mm active area. Figure 4(a) shows 3 projections out of the 500 projections acquired by the camera across a horizontal range of 10 cm. As shown in this figure, the relative positions of the digits change only along the horizontal axis (but not along the vertical axis) as a function of the location of the projection in the entire set of projections.

Similar to the simulation presented in Section 4, each of the acquired projections was multiplied, according to Eqs. (1) and (2) by a 1-D quadratic phase function, and the result was summed to a single column in the 1-D modified Fresnel hologram of the 3-D scene. Figure 4(b) shows the magnitude and the phase of the hologram obtained from this procedure.

Digital reconstruction of the 3-D scene recorded into the hologram was obtained by convolving the hologram with a 1-D quadratic phase function according to Eq. (8). Figure 4(c) shows six chosen planes reconstructed along the optical axis. As before, in each plane, a different digit is in focus, whereas the other five digits are out of focus. This behavior validates the volumetric information encoded into the experimentally obtained hologram.

Figure 4(d) shows the best in-focus reconstructed planes, resampled on the horizontal axis by M/M_x (as it was performed for the simulation results described in Section 4). Following the resampling process, the aspect ratios of the reconstructed objects in each of the best in-focus planes are similar to the aspect ratios of the objects in the original 3-D scene.

According to Eq. (12), the axial magnification of the obtained hologram is directly dependent on both the axial position of the considered object and its size. The dashed curve in Fig. 5 illustrates the experimental values of $\bar{z}_r$ versus $\bar{z}_s$. The solid curve in Fig. 5 illustrates the predicted graph according to Eq. (11), where the experimental parameters used are $b = 0.0016$ pixel^{-2}, $\gamma = 1$ pixel, and $\alpha = 312/(500M_{\max})$ pixel. Both values $\bar{z}_s$ and $\bar{z}_r$ were measured

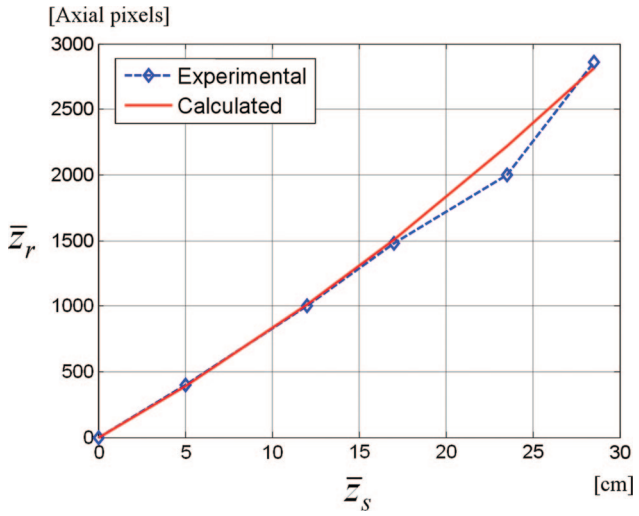

Fig. 5. (Color online) Graph of the axial size of the reconstructed object $\bar{z}_r$ versus the axial size of the observed object $\bar{z}_s$. Solid curve—predicted (calculated) curve; dashed curve—based on the experimental results. The diamond points represent each one of the six object planes.

from the first plane of the digit 1 to the rest of the five planes. The resemblance between the two curves indicates that Eq. (11) and consequently Eq. (12) describe well the behavior of the axial magnification of this hologram.

6. Conclusions

We have presented a direct method for obtaining MVP modified Fresnel holograms of real existing 3-D objects illuminated by incoherent white light. The hologram has been processed directly from the MVPs of the 3-D scene, without obtaining the Fourier hologram first, as performed in the past. The proposed MVP method is more accurate than the former MVP Fresnel holography method since no redundant transformations or approximations are needed. Moreover, the new method is especially useful for high-resolution MVP Fresnel holograms, since it can spare a lot of redundant calculations performed in the former MVP methods. Video holography is a possible application of the proposed method, since the digital calculations of the hologram synthesis can be performed in real time.

Other kinds of directly generated MVP holograms are most likely possible and probably will be explored in the future. This concept helps eliminate redundant digital calculations and thus makes the entire hologram generation process more accurate and faster. Problems such as anisotropic radiation and partial occlusions in the recorded 3-D scene are beyond the scope of the present study and will be addressed in future research.

References

1. Y. Li, D. Abookasis, and J. Rosen, "Computer-generated holograms of three-dimensional realistic objects recorded without wave interference," Appl. Opt. **40,** 2864–2870 (2001).
2. D. Abookasis and J. Rosen, "Computer-generated holograms of three-dimensional objects synthesized from their multiple angular viewpoints," J. Opt. Soc. Am. A **20,** 1537–1545 (2003).
3. Y. Sando, M. Itoh, and T. Yatagai, "Holographic three-dimensional display synthesized from three-dimensional Fourier spectra of real existing objects," Opt. Lett. **28,** 2518–2520 (2003).
4. T. Yatagai, "Stereoscopic approach to 3-D display using computer-generated holograms," Appl. Opt. **15,** 2722–2729 (1976).
5. D. Abookasis and J. Rosen, "Three types of computer-generated hologram synthesized from multiple angular viewpoints of a three-dimensional scene," Appl. Opt. **45,** 6533–6538 (2006).
6. N. T. Shaked, J. Rosen, and A. Stern, "Integral holography: white-light single-shot hologram acquisition," Opt. Express **15,** 5754–5760 (2007).
7. B. Katz, N. T. Shaked, and J. Rosen, "Synthesizing computer generated holograms with reduced number of perspective projections," Opt. Express **15,** 13250–13255 (2007).
8. Y. Sando, M. Itoh, and T. Yatagai, "Full-color computer-generated holograms using 3-D Fourier spectra," Opt. Express **12,** 6246–6251 (2004).
9. J. W. Goodman, *Introduction to Fourier Optics,* 2nd ed. (McGraw-Hill, 1996), pp. 67 and 353.